

Dynamics of cubic-tetragonal phase transition in KNbO_3 perovskite

S.N. Gvasaliya*

Laboratory for Neutron Scattering ETHZ & Paul-Scherrer Institut CH-5232 Villigen PSI Switzerland

B. Roessli

Laboratory for Neutron Scattering ETHZ & Paul-Scherrer Institut CH-5232 Villigen PSI, Switzerland

R.A. Cowley

Clarendon Laboratory, Oxford University, Parks Road, Oxford OX1 3PU, UK

S.G. Lushnikov

Ioffe Physical Technical Institute, 26 Politekhnicheskaya, 194021, St. Petersburg, Russia

A. Choubey and P. Gunter

Nonlinear Optics Laboratory, ETH Honggerberg, CH-8093 Zürich, Switzerland

(Dated: November 4, 2018)

The low-energy part of the vibration spectrum in KNbO_3 was studied by cold neutron inelastic scattering in the cubic phase. In addition to acoustic phonons, we observe strong diffuse scattering, which consists of two components. The first one is quasi-static and has a temperature-independent intensity. The second component appears as quasi-elastic scattering in the neutron spectrum indicating a dynamic origin. From analysis of the inelastic data we conclude that the quasi-elastic component and the acoustic phonon are mutually coupled. The susceptibility associated with the quasi-elastic component grows as the temperature approaches T_C .

PACS numbers: 77.80.-e, 61.12.-q, 63.50.+x, 64.60.-i

ABO_3 perovskites form a class of important materials, in part because of potential technical applications but also as fundamental interest in the physics of phase transitions [1, 2]. At sufficiently high temperatures many of these perovskites have O_h^1 cubic symmetry and structural phase transitions can take place as the temperature is lowered. Well-known examples are *e.g.* the cubic-tetragonal phase transition in SrTiO_3 ($T_C \approx 105$ K) or in BaTiO_3 ($T_C \approx 425$ K) (for a review see Ref. [3]). There are, however, ABO_3 perovskites which were less studied. An example is the first-order cubic-tetragonal phase transition in KNbO_3 which occurs at $T_C \approx 683$ K when cooling the crystal from above the transition temperature [4].

The mechanism of the cubic-tetragonal (CT) phase transition in KNbO_3 is still controversial. Whereas well-defined soft phonon modes with frequency varying with temperature have been detected in many materials close to T_C [1 - 3], only an over-damped excitation has been observed in cubic KNbO_3 with neutron scattering and it was suggested that the nature of the C-T phase transition in that compound is similar to the displacive C-T transition in BaTiO_3 [5, 6]. On the other hand, two coexisting and essentially uncoupled modes are inferred from analysis of optical data in the cubic phase of KNbO_3 : a relaxation mode and a soft phonon, with the relaxation process driving the C-T phase transition [7].

We re-investigated the low energy part of the vibration spectrum in KNbO_3 under improved resolution condi-

tions first to try to elucidate the mechanism of the phase transition in this crystal and second to check whether the diffuse scattering found in Ref.[8] is of static or dynamic origin. The inelastic cold-neutron scattering measurements reported here were performed with the three-axis spectrometer TASP, located at the neutron spallation source SINQ (Paul Scherrer Institute, Switzerland). A large single crystal of KNbO_3 ($\sim 20 \text{ cm}^3$, mosaic $\sim 80'$) was mounted into an ILL-type furnace. To decrease the level of incoherent background the sample holder was made from pure niobium. The crystal was aligned in the (h k 0) scattering plane. The measurements were performed in the temperature range 727 K - 1030 K. The (002) reflection of pyrolytic graphite (PG) was used to monochromate and analyze the incident and scattered neutron beams, respectively. The spectrometer was operated in the constant final-energy mode with $k_f = 1.97 \text{ \AA}^{-1}$. A PG filter was used to remove higher-order wavelengths. The horizontal collimation was $10'/\text{\AA} - 80' - 80' - 80'$. With that configuration the energy resolution at zero energy transfer is $\sim 0.4 \text{ meV}$. By monitoring the position and intensity of the (1, 1, 0) Bragg peak, the temperature of the cubic-tetragonal phase transition upon cooling was found at $T_C = 684 \pm 2 \text{ K}$, in close agreement with published data [4, 6]. The temperature of the sample was controlled by two thermocouples. The temperature gradient through the sample did not exceed 15 K.

Before analyzing the inelastic neutron spectra quan-

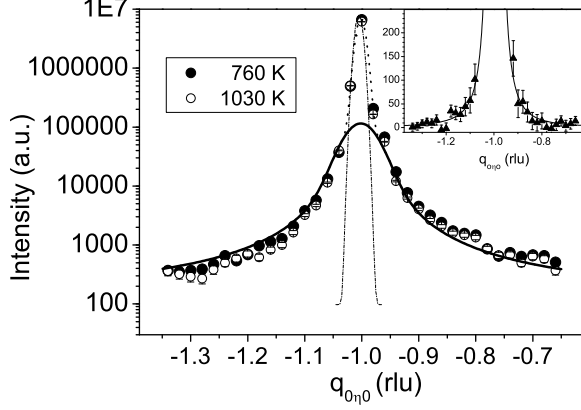


FIG. 1: Profiles of elastic scans in the $(0\eta 0)$ direction at $T = 760$ K and $T = 1030$ K. Raw data are shown by circles. The dotted line is the result of fits as described in the text. The bold line shows the Lorentzian profile, the dashed-dotted line stands for the intense and narrow Bragg peak. The intensity is given in a logarithmic scale. The insert shows the difference of the elastic scans $I(T = 760\text{K}) - I(T = 1030\text{K})$ fitted with Eq. 1. 1 rlu corresponds to 1.57 \AA^{-1} .

titatively, it is convenient to address the q -dependence of the elastic neutron response. Figure 1 shows representative elastic scans along the $(1, 1 \pm q, 0)$ direction at $T = 760$ K and 1030 K, respectively. This intense and broad scattering is similar to the diffuse scattering observed in KNbO_3 by Guinier et al. [8] using X-rays and reflects the presence of atomic disorder in the perovskite cell. In KNbO_3 atomic disorder yields diffuse scattering along the $[100]$ direction both in the X-ray and neutron diffraction patterns. Here we approximate the line-shape of the neutron diffuse scattering intensity by a Lorentzian profile:

$$A(q) = \frac{1}{\pi} \frac{I_0}{(q - q_0)^2 + \kappa^2} \quad (1)$$

where q_0 is the position in reciprocal space; κ the inverse of the correlation length ξ and I_0 yields the integrated intensity. From a fit to the elastic data at $T = 1030$ K we obtain $\xi = 64 \pm 6 \text{ \AA}$. It turns out that the shape and intensity of the diffuse scattering measured in the $(2, 0, 0)$ Brillouin zone (BZ) does not depend on temperature (see insert of Fig. 2). This is in agreement with the results of Ref. [8] where the intensity of the diffuse scattering is found to be temperature independent in the cubic phase and to decrease abruptly by $\sim 30\%$ immediately below T_C . On the other hand, it turns out that the intensity of the diffuse scattering measured along $(1, 1 \pm q, 0)$ slowly decreases when increasing the temperature from T_C . This suggests that in that BZ and for temperatures relatively close to T_C , the diffuse scattering consists of

two Lorentzian components (see inset of Fig. 1).

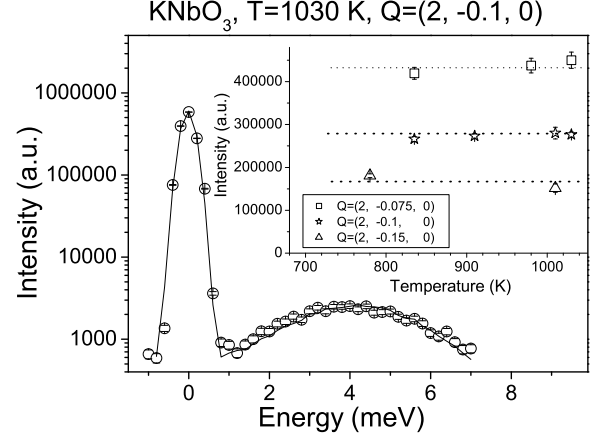


FIG. 2: Neutron scattering spectrum from KNbO_3 at 1030 K. Raw data are shown by open circles. The solid line is the result of fit as described in the text. The intensity is given in a logarithmic scale. The apparent width of the phonon peak is due to the resolution effects. The insert shows the temperature and the q dependences of the intensity of the central peak. 1 rlu = 1.567 \AA^{-1} .

We turn now to the analysis of the inelastic neutron scattering spectra. Figure 2 shows an example of a constant- q scan taken at $\mathbf{Q} = (2, -0.1, 0)$ and $T = 1030$ K. The spectrum contains an inelastic peak at $\hbar\omega = 4 \text{ meV}$ from the transverse acoustic (TA) phonon and a narrow peak centered around zero energy transfer. To analyze the data quantitatively, we hence modeled the neutron scattering intensity $I(\mathbf{Q}, \omega)$ in the following way:

$$I(\mathbf{Q}, \omega) = S(\mathbf{Q}, \omega) \otimes R(\mathbf{Q}, \omega) + B \quad (2)$$

The symbol \otimes stands for the 4-D convolution with the spectrometer resolution function $R(\mathbf{Q}, \omega)$ [9]; B denotes the background level; $S(\mathbf{Q}, \omega)$ is the neutron scattering function which is related to the imaginary part of the dynamical susceptibility $\chi''(\mathbf{Q}, \omega)$ through

$$S(\mathbf{Q}, \omega) = \frac{[n(\omega) + 1]}{\pi} \chi''(\mathbf{Q}, \omega) \quad (3)$$

with the temperature factor $[n(\omega) + 1] = [1 - \exp(-\omega/T)]^{-1}$. We approximate the central peak by a δ -function in energy

$$S_{CP} = A(q) \delta(\omega) \quad (4)$$

with $A(q)$ given by Eq. 1. The line-shape of the acoustic phonon is given by the usual damped-harmonic oscillator (DHO)

$$\chi_{DHO}(\mathbf{q}, \omega) = (\Omega_q^2 - i\gamma_q\omega - \omega^2)^{-1}. \quad (5)$$

In Eq. 5, γ_q is the damping and $\Omega_q = \sqrt{\omega_q^2 + \gamma_q^2}$ with $\omega_q = c \cdot q$ [10] is the renormalized frequency of the acoustic phonons. For small values of momentum transfers q , a linear dispersion for the acoustic phonon branch is a reasonable approximation and the phonon damping approximately follows a dq^2 -dependence [11]. The scattering function used to fit the neutron data then reads

$$S(\mathbf{Q}, \omega) = S_{CP}(\mathbf{Q}, \omega) + \frac{[n(\omega) + 1]}{\pi} f_1^2 \chi_{DHO}''(\mathbf{Q}, \omega) \quad (6)$$

where $\mathbf{Q} = \mathbf{q} + \boldsymbol{\tau}$ is the neutron scattering vector and $\boldsymbol{\tau}$ a reciprocal lattice vector; f_1 is the structure factor of the acoustic phonon. As shown in Fig.2, Eqs. 1-6 parameterize the experimental data in the $(2, 0, 0)$ BZ well. The central peak is resolution-limited and temperature-independent. The acoustic phonon branch has a stiffness $c = 28 \pm 1.3 \text{ meV} \cdot \text{\AA}^2$ and the damping is small at low q , $\gamma_q = dq^2$ with $d = 55 \pm 6 \text{ meV} \cdot \text{\AA}^2$ ($0.05 < q < 0.15 \text{ (rlu)}$). In the temperature range $750 \text{ K} < T < 1030 \text{ K}$ no qualitative change in the dispersion of the acoustic phonon was observed for data taken along $(2, q, 0)$ ($|q| < 0.15 \text{ (rlu)}$).

On the contrary, for temperatures below $T=1030 \text{ K}$ an additional component is observed in the inelastic spectra for constant- q scans in the $(1, 1, 0)$ BZ. For means of comparison, Fig. 3 shows two representative neutron scattering spectra measured in the $(1, 1, 0)$ BZ at $T=1030 \text{ K}$ and $T=727 \text{ K}$, respectively. At $T = 1030 \text{ K}$ the spectrum consists of two components - a central peak (CP) and a phonon response around $\hbar\omega = 4 \text{ meV}$. However, as the temperature is lowered to $T=727 \text{ K}$, additional quasielastic scattering (QE) appears along $(1, 1 \pm q, 0)$ direction. The intensity of this quasi-elastic scattering grows when approaching T_C . From the above discussion we conclude that in the $(1, 1, 0)$ BZ, the inelastic neutron spectra consist of three contributions: a central peak, quasi-elastic and phonon scattering. To describe the quasi-elastic scattering we introduce a Debye-like relaxation function

$$\chi_{q-el}(\mathbf{q}, \omega) = \frac{\chi(0, T)}{1 + q^2/\kappa^2} \cdot (1 - i\omega/\Gamma_q)^{-1}, \quad (7)$$

$\chi(0, T)$ is the temperature dependent static susceptibility; κ the inverse of the correlation length and $\Gamma_q = \Gamma_0 + Dq^2$. Taking into account the quasi-elastic scattering modifies the neutron cross-section to

$$S(\mathbf{Q}, \omega) = S_{CP}(\mathbf{Q}, \omega) + \frac{[n(\omega) + 1]}{\pi} [f_1^2 \chi_{DHO}''(\mathbf{Q}, \omega) + f_2^2 \chi_{q-el}''(\mathbf{Q}, \omega)], \quad (8)$$

However, the scattering function given in Eq. 8 fails in reproducing the experimental data in the $(1, 1, 0)$ BZ for $T < 1030 \text{ K}$. For example Fig. 3 shows an inelastic spectrum at $T=727 \text{ K}$ and $\mathbf{Q}=(1, 1.075, 0)$ where a qualitative change in the phonon line-shape accompanied by a shift in the position of the phonon peak is observed. These two effects suggest that coupling between

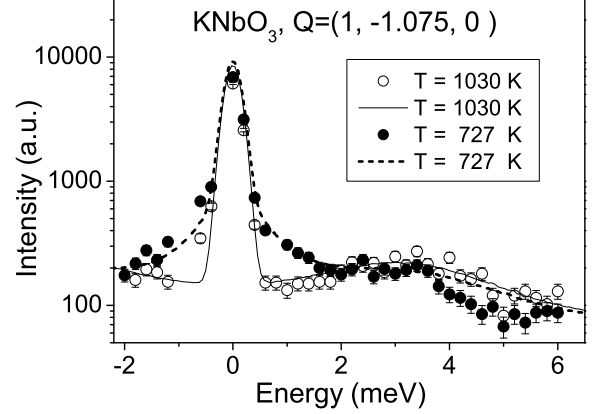


FIG. 3: Neutron scattering spectrum from KNbO_3 at $T=1030$ and 727 K , respectively. The solid and dashed line are the results of fit as described in the text. To emphasize the QE component the intensity is given in a logarithmic scale. Note the pronounced change in the phonon line-shape at lower temperature.

the quasi-elastic component and the acoustic phonons becomes important as the temperature approaches T_C .

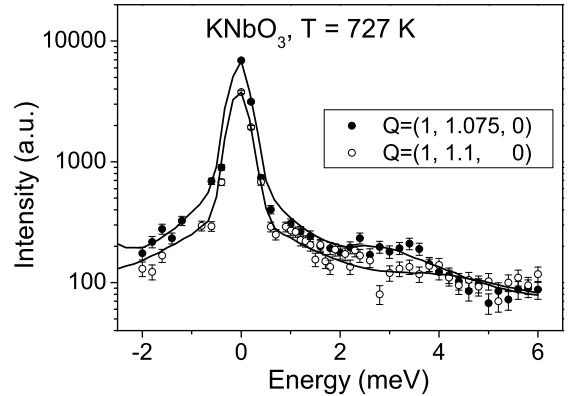


FIG. 4: Observed and fitted inelastic neutron intensities taken in the $(1, 1, 0)$ BZ at $T=727 \text{ K}$. Fitted curves were obtained with Eq. 10. Intensity is given in a logarithmic scale.

The dynamical susceptibility for two coupled excitations was considered in details in Refs. [3, 12, 13] and is given by

$$\chi_{CM}(\mathbf{Q}, \omega) = \frac{f_1^2 \chi_1 + f_2^2 \chi_2 + 2\lambda f_1 f_2 \chi_1 \chi_2}{1 - \lambda^2 \chi_1 \chi_2} \quad (9)$$

where $\chi_i \equiv \chi_i(\mathbf{Q}, \omega)$, $i = 1, 2$ are the dynamical susceptibilities of the uncoupled phonon and QE component,

respectively. In the following we take f_i as real constants since in KNbO_3 all the atoms are situated on centers of symmetry. The interaction term is $\lambda \equiv \lambda(q, \omega) = (g_r + i\omega g_i) q^2$. Finally, the scattering function reads:

$$S(\mathbf{Q}, \omega) = S_{CP}(\mathbf{Q}, \omega) + \frac{[n(\omega) + 1]}{\pi} \chi''_{CM}. \quad (10)$$

In order to obtain a good agreement between Eq. 10 and the neutron spectra, it was necessary to fit the complete set of data ($0 < q < 0.2$) taken at a given temperature simultaneously. Figures 4 and 5 show the results of such calculations for $T=727$ K and $T=760$ K. We obtain $g_r = 20 \pm 3 \text{ meV}^2 \cdot \text{\AA}^2$ and $g_i = 95 \pm 6 \text{ meV} \cdot \text{\AA}^2$. Introduction of a coupling between the QE and acoustic modes has two consequences. First, Eq. 9 yields a better description of the line-shape of the inelastic neutron spectra. Second, $\chi''_{CM}(\mathbf{Q}, \omega)$ is enhanced at low energy transfers. Further, we obtained $\Gamma_0 = 0.19 \pm 0.05 \text{ meV}$ and $D = 44 \pm 4 \text{ meV} \cdot \text{\AA}^2$ for the damping of QE component. As discussed above, both the CP and the

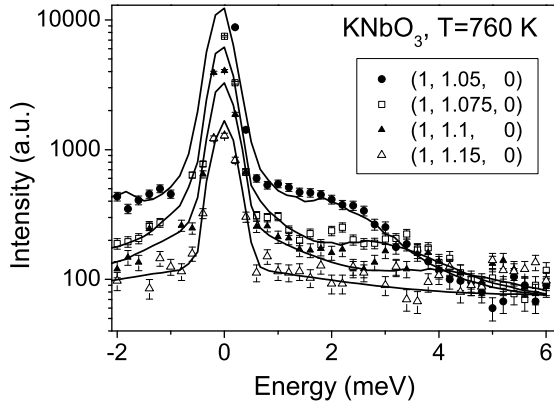


FIG. 5: Observed and fitted inelastic neutron intensities taken in the (1, 1, 0) BZ at $T=760$ K. Fitted curves were obtained with Eq. 10. Intensity is given in a logarithmic scale.

line-shape of the acoustic phonons are temperature independent in the (2, 0, 0) BZ. Hence, to fit the data measured in the (1, 1, 0) BZ as a function of temperature, we fixed the parameters of the CP and the acoustic phonons. The only parameter left to describe the temperature dependence of the neutron spectra is the susceptibility of QE scattering $\chi(0, T)$. As shown in Fig. 5 the intensity of the quasi-elastic component is a maximum close to T_C and decreases continuously with increasing temperature. The temperature dependence of $\chi(0, T)$ follows approximately the Curie-Weiss law $\propto 1/(T - T_0)$ with $T_0 = 615 \pm 23$ K in good agreement with the value deduced from dielectric measurements $T_0 = 633 \pm 5.9$ K (Ref. [14]), and $T_0 = 615$ K (Ref. [15]). This suggests that the cubic-tetragonal transition in KNbO_3 is driven

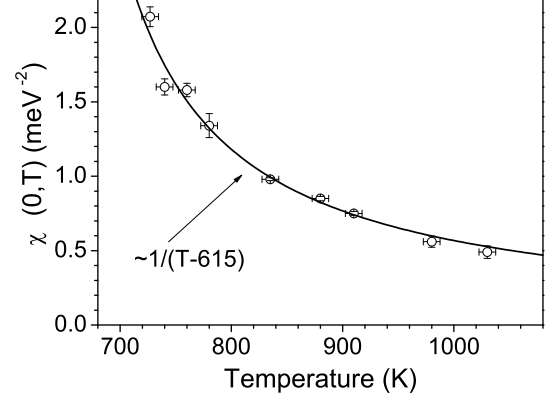


FIG. 6: Temperature dependence of the susceptibility of the QE component. The solid line is a fit to the data as explained in the text.

by the quasi-elastic relaxational excitation. The intensity of the quasi-elastic component is strong in the (1,1,0) zone and has a small intensity in the (2,0,0) Brillouin zone, which indicates that the relaxation mode is due to correlated atomic motion of optical character. However, at all q and temperatures we did not observe that the relaxation mode evolves into an under-damped optic phonon branch. Thus, we conclude that QE scattering in KNbO_3 is not due to an usual overdamped soft phonon but is related to disorder in the lattice.

To summarize, we measured the low-energy part of the vibration spectrum of KNbO_3 in the cubic phase with inelastic neutron scattering. We find a coexistence of a static and a quasi-elastic component. The static component appears to correspond with static disorder in the cubic cell and is temperature independent in agreement with X-rays results [5]. The quasi-elastic component is coupled with the acoustic phonon branch and its intensity follows the Curie-Weiss law well.

This work was performed at the spallation neutron source SINQ, Paul Scherrer Institut, Villigen (Switzerland) and was partially supported by RFBR grant 02-02-17678. P. Günter and A. Choubey acknowledge partial support by the Swiss National Science Foundation.

* On leave from Ioffe Physical Technical Institute, 26 Politekhnicheskaya, 194021, St. Petersburg, Russia

- [1] G. A. Smolenskii, V. A. Bokov, V. A. Isupov, N. N. Krainik, R. E. Pasynkov, and N. K. Yushin, *Ferroelectrics and Related Materials* (New York, Gordon and Breach, 1984).
- [2] M. E. Lines and A. M. Glass, *Principles and applications of ferroelectrics and related materials* (Oxford, Clarendon

- Press, 1977).
- [3] A. D. Bruce and R. A. Cowley, *Structural phase transitions* (London, Taylor & Francis, 1981).
 - [4] G. Shirane, H. Danner, A. Pavlovic, and R. Pepinsky, Phys. Rev. **93**, 672 (1954).
 - [5] A.C. Nunes, J.D. Axe and G. Shirane, Ferroelectrics **2**, 291 (1971).
 - [6] M. Holma and Haydn Chen, J. Phys. Chem. of Solids **57**, 1465 (1996).
 - [7] M. D. Fontana, A. Ridah, G. E. Kugel, and C. Carabatos-Nedelec, J. Phys. C **21**, 5853 (1988).
 - [8] R. Comes, M. Lambert, and A. Guinier, Acta Crystallogr. **A26**, 244 (1970).
 - [9] M. Popovich, Acta Cryst. **A31**, 507 (1975).
 - [10] B. Fåk and B. Dorner, Physica **B234**, 1107 (1997).
 - [11] A.A. Maradudin and A.E. Fein Phys. Rev. **128**, 2589 (1962).
 - [12] R.K. Wehner and E.F. Steigmeier, RCA Review **36**, 70 (1975).
 - [13] G. J. Coombs and R. A. Cowley, J. Phys. C **6**, 121 (1973).
 - [14] S. Triebwasser, Phys. Rev. **101**, 993 (1956).
 - [15] V.K. Yanovskii, Sov. Phys. Solid State **22**, 1284 (1980).